Electronic Supplementary Material (ESI) for Nanoscale.

SUPPORTING INFORMATION

Tuning the sensitivity of lanthanide activated NIR nanothermometers in the biological windows

P. Cortelletti[a], A. Skripka[b], C. Facciotti[a,c¶], M. Pedroni[a], G. Caputo[d], N. Pinna[e], M. Quintanilla[b,f], A. Benayas[b,g], F. Vetrone[b,h,i]*, A. Speghini[a]*

a. Nanomaterials Research Group, Dipartimento di Biotecnologie, Università di Verona and INSTM, UdR Verona, Strada Le Grazie 15, I-37134 Verona, Italy.
b. Centre Énergie, Matériaux et Télécommunications, Institut National de la Recherche Scientifique, Université du Québec, Varennes, QC J3X 1S2, Canada
c. Wageningen University & Research, Axis Y, Bornse Weilanden 9, 6708, Wageningen, The Netherlands [current address].
d. Smart Materials, Istituto Italiano di Tecnologia, Via Morego 30, 16163 Genova, Italy
e. Institut für Chemie, Humboldt Universität zu Berlin, Brook-Taylor-Straße 2, 12489 Berlin, Germany.
f. BioNanoPlasmonics Laboratory, CIC biomaGUNE, Paseo de Miramón 182, Donostia [current address]
g. Department of Physics and CICECO – Aveiro Institute of Materials, University of Aveiro, 3810-193, Aveiro, Portugal [current address]
h. Centre for Self-Assembled Chemical Structures, McGill University, Montréal, Québec H3A 2K6, Canada
i. Institute of Fundamental and Frontier Science, University of Electronic Science and Technology of China, Chengdu 610051, China

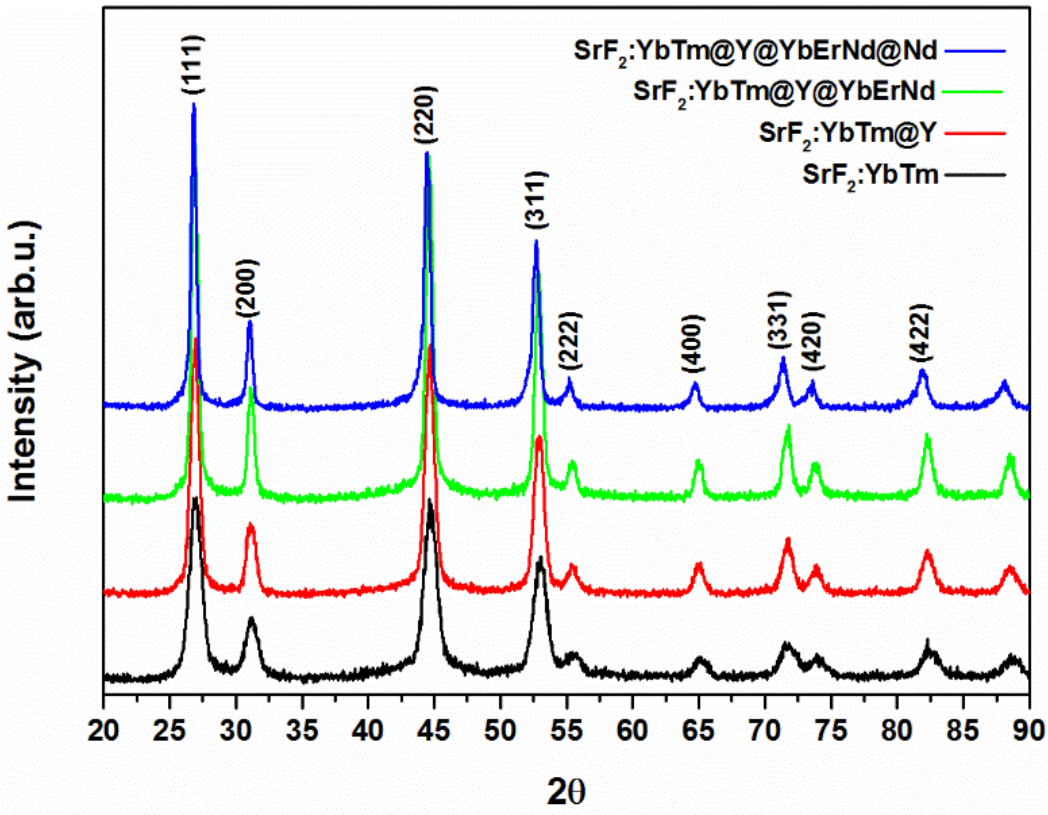

Figure SI1. XRPD patterns for MNPs doped with 2 % Er^{3+} for subsequent shell formation.

2% Er^{3+} MNP	core	c@s	c@s@s	c@s@s@s
XRD	7.2 ± 0.2	10.0 ± 0.2	13.7 ± 0.3	16.4 ± 0.6

Table SI1. Average particle size for the MNPs doped with 2% Er^{3+} after consecutive reaction steps evaluated by XRPD.

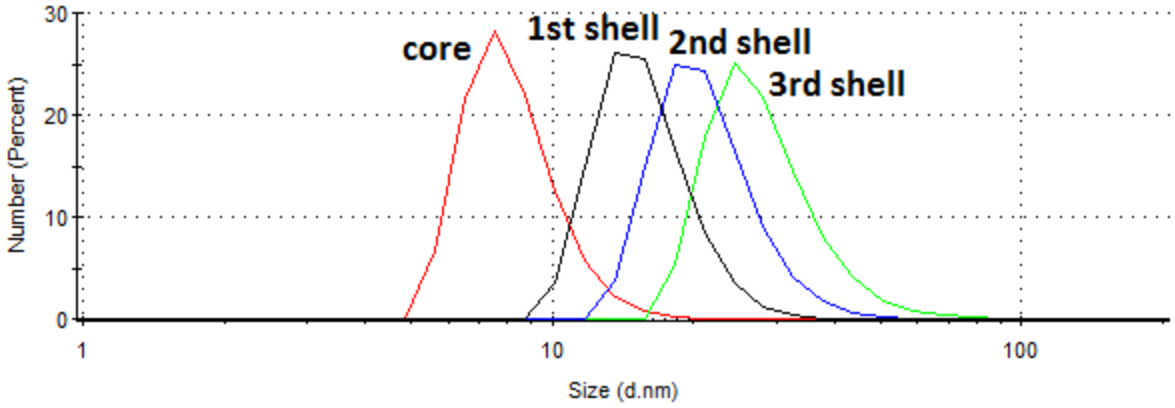

Figure SI2. Hydrodynamic average size measured by DLS for MNPs with 2% Er^{3+}.

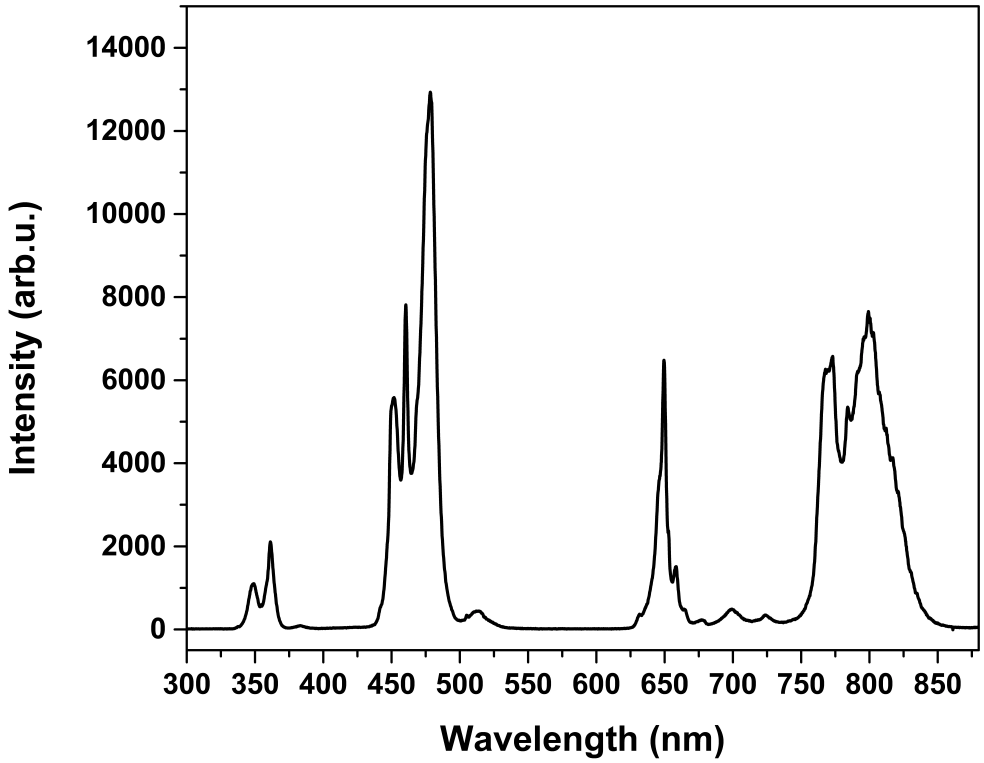

Figure SI3. UC emission upon 980 nm excitation of the core SrF_2:YbTm NPs.

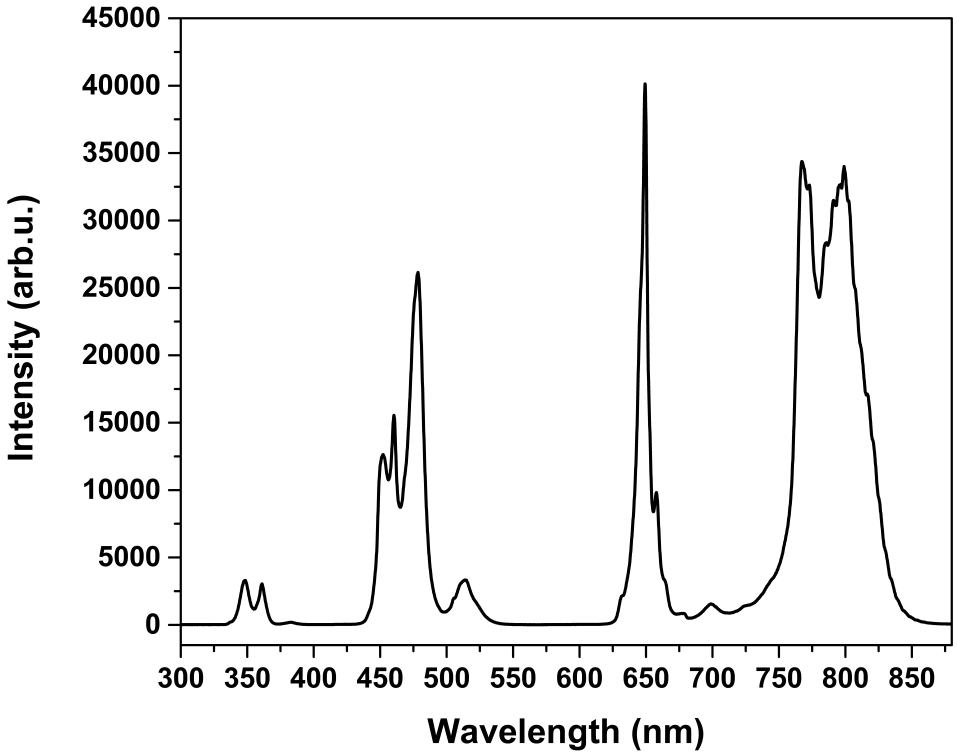

Figure SI4. UC emission upon 980 nm excitation of the core@shell NPs, SrF_2:YbTm@Y. An increase in the 650 nm and 800 nm emission bands can be noticed, with an increase of the signal/noise ratio, due to an overall intensification of the emission.

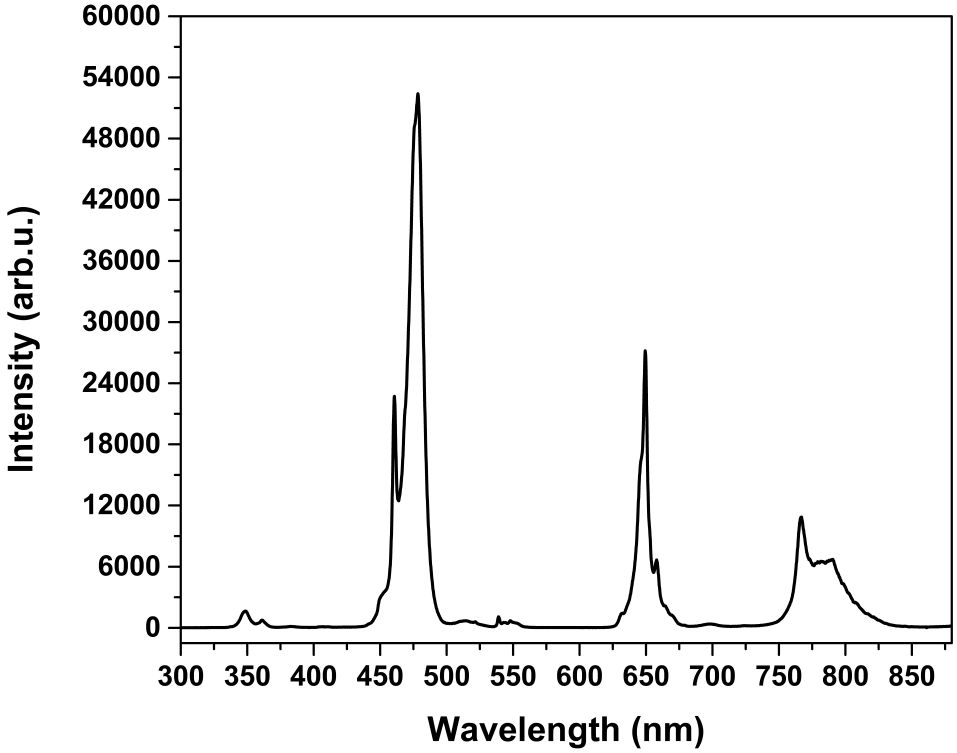

Figure SI5. UC emission upon 980 nm excitation of the core@shell@shell NPs, SrF_2:YbTm@Y@YbEr(1%)Nd. An increase in Tm^{3+} emission band at 460 nm can be noticed, probably due to the lower interaction of Tm^{3+} ions with the solvent, since Tm^{3+} ions are located only in the core of the MNPs. A typical Er^{3+} ions emission band can be seen at 550 nm, the low intensity is due to a quenching induced by the solvent.

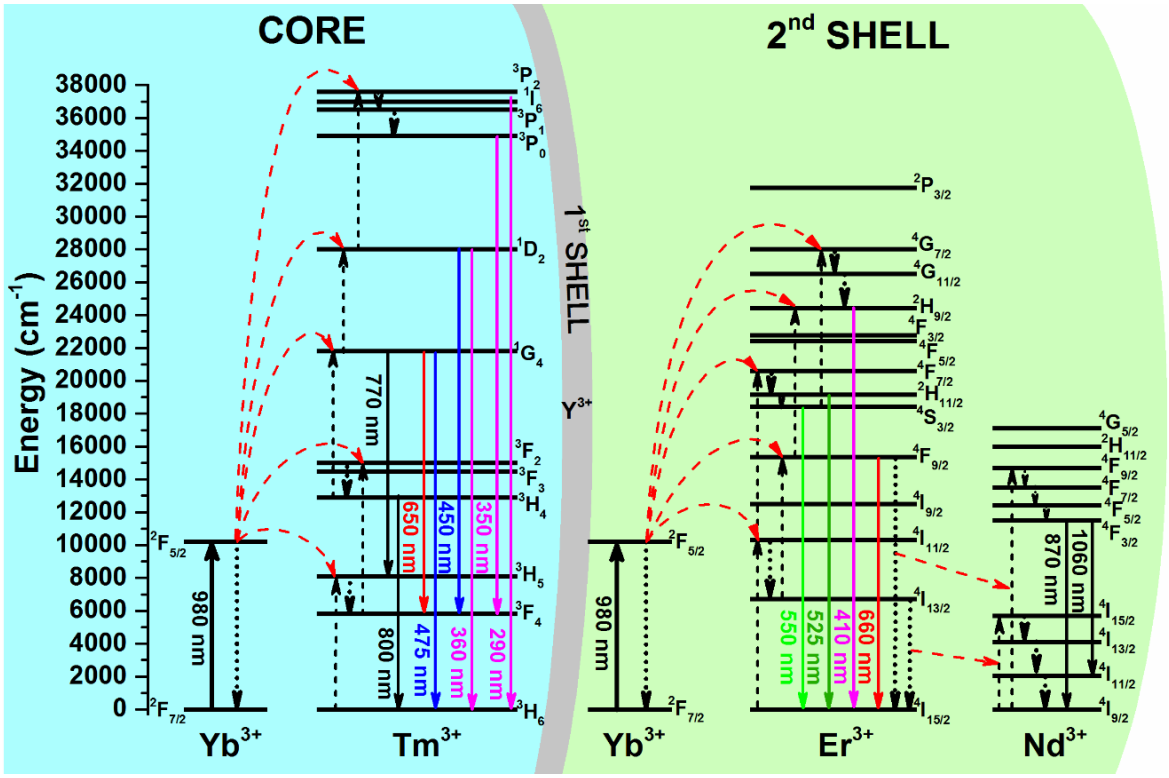

Figure SI6. Energy transfer and emission processes for the MNPs upon 980 nm excitation.

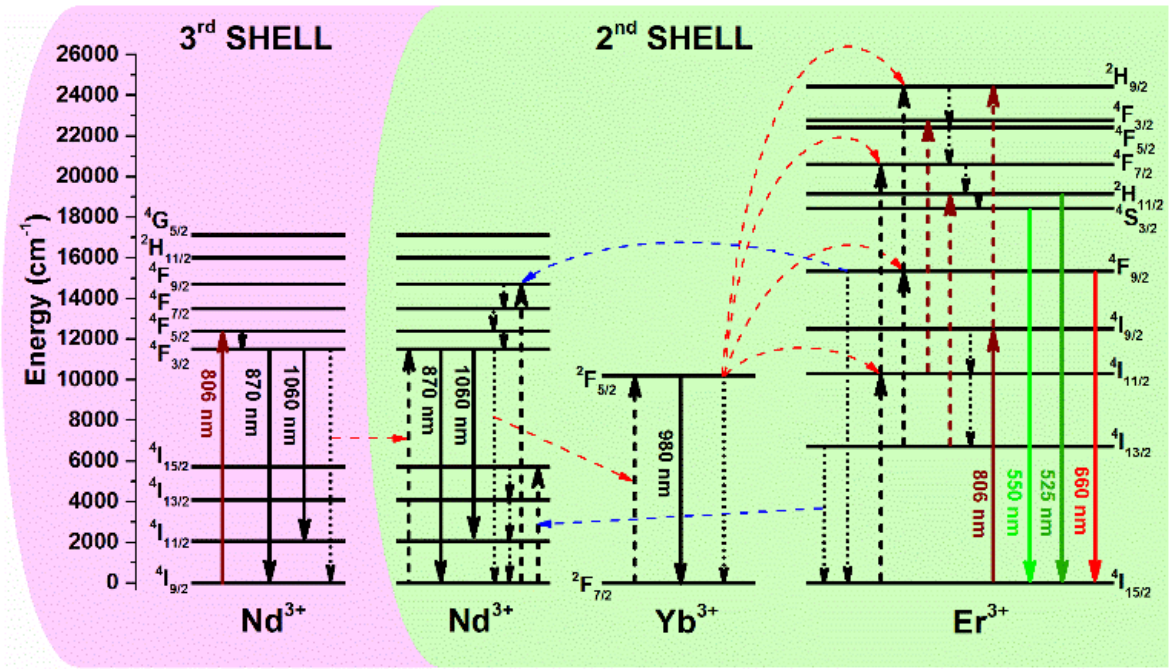

Figure SI7. Energy transfer (ET) and emission processes for MNPs upon 806 nm excitation. Brown, ascending solid arrows represent laser excitation. Dotted descending black arrows represent non-radiative de-excitation. Descending solid arrows represent emission. Ascending dashed arrows represent energy absorption (ascending brown dashed arrows represent ESA of 806 nm radiation). Red dashed arrows represent ET. Blue dashed arrows represent $Er^{3+} \rightarrow Nd^{3+}$ ET.

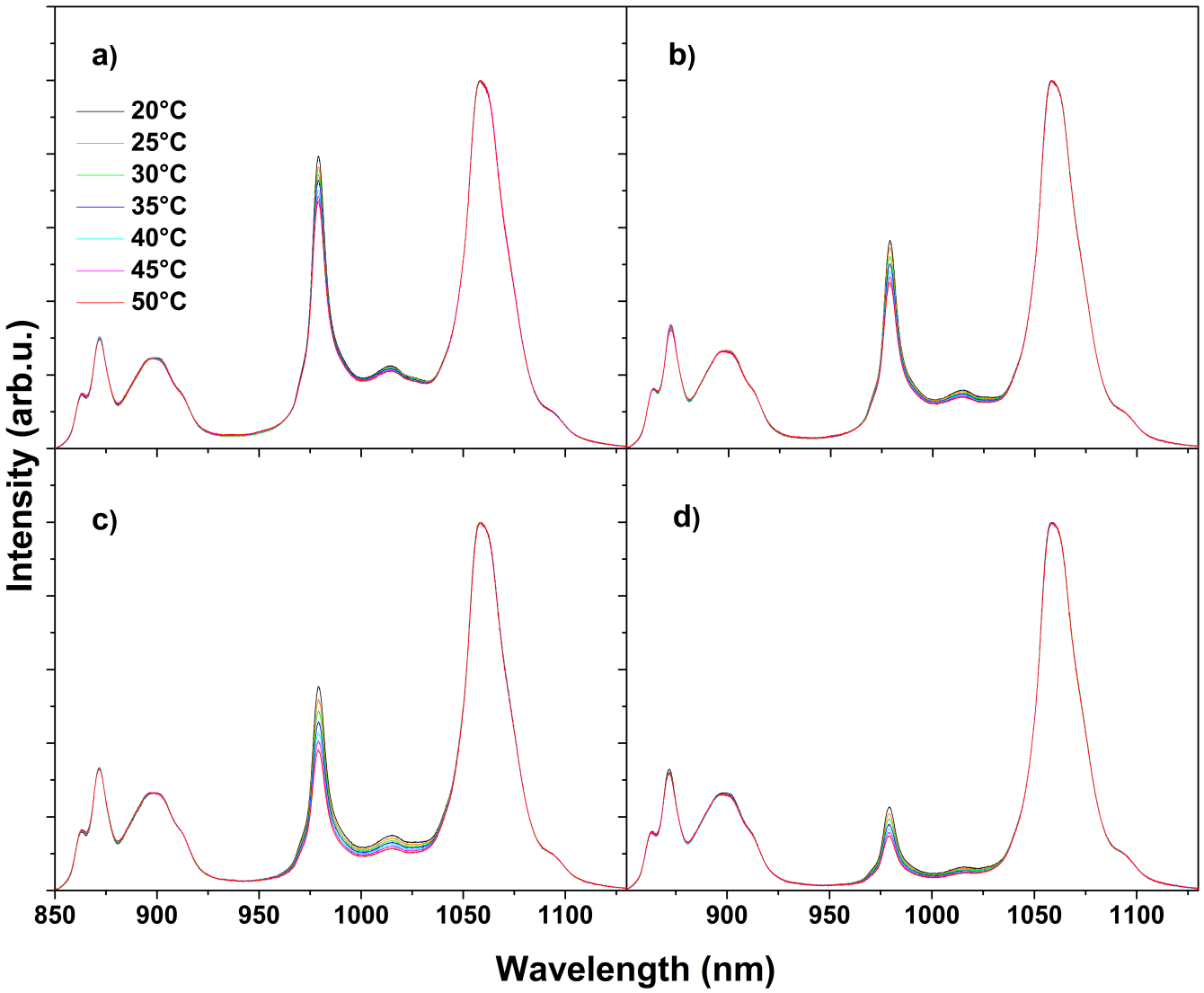

Figure SI8. Thermometric measurements of the MNPs with different Er^{3+} concentration in the second shell. Er^{3+} 0.2% in **a)**, 1% in **b)**, 4% in **c)**, 8% in **d)**.

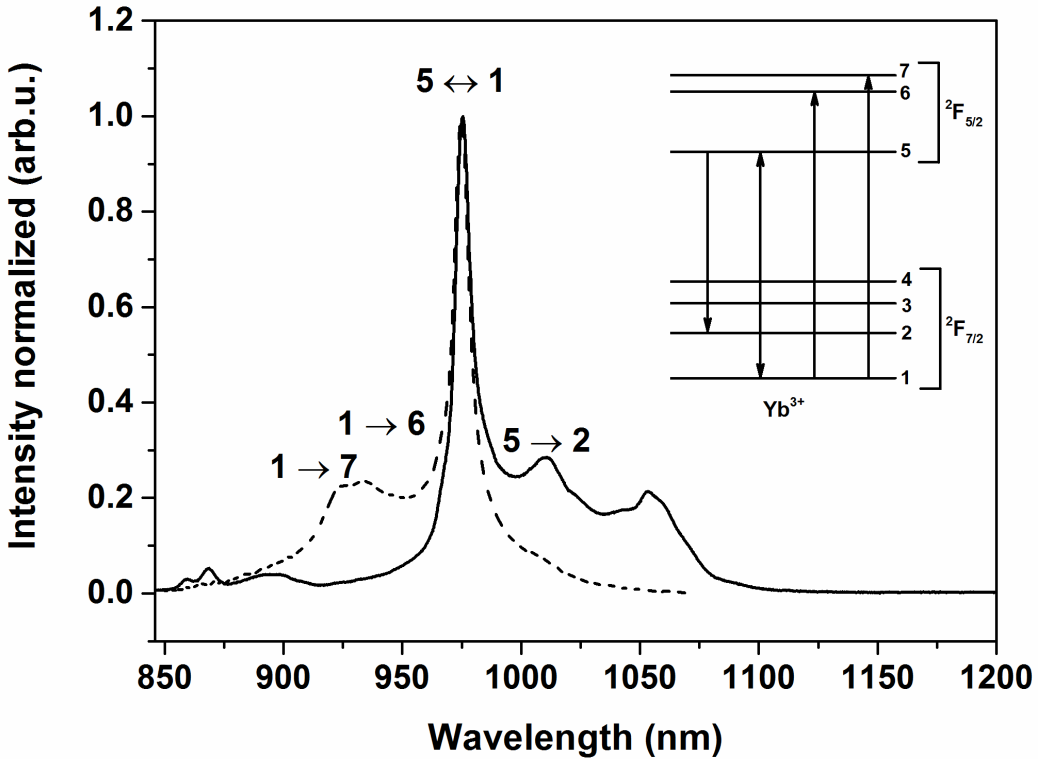

Figure SI9. MNPs NIR absorption (dashed line), and emission (solid line) upon 806 nm excitation. In the inset the Stark levels of the Yb^{3+} ions are highlighted. An increasing thermal population of the 6 and 7 levels allows the increase of the Nd^{3+}←Yb^{3+} back ET process.